# Smart Flexible Camera Sheet: Ultra-thin Semantic-guided Cooperative Micro-camera Array

Kari Van Grinsven, Shiwei Zhou, Zhengyang Lou, Liangzhi Lai, John Jansky, Alireza Ousati Ashtiani, Jae-Jun Kim, Yu Hen Hu, and Hongrui Jiang

University of Wisconsin - Madison

## OBJECTIVE

Develop a 'smart' flexible sheet with an integrated micro-camera array, wherein the cameras can individually or collectively target and track objects at different angles and distances.

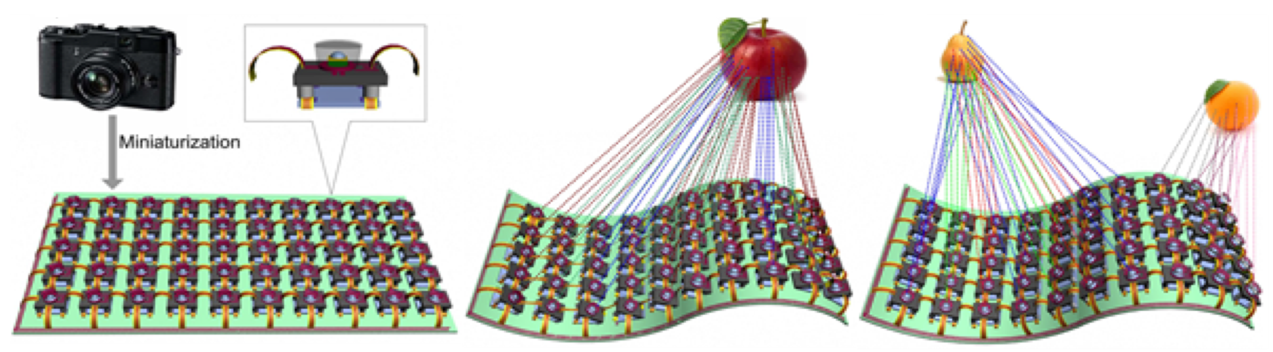


Fig 1. (a) Schematics of the proposed camera sheet that is formed with a micro-camera array. The camera sheet is flexible and can be installed on or embedded in any planar or curved surface. Each micro-camera can be re-oriented on demand to change its viewing direction. Also, the operation of the micro-cameras is highly coordinated; (b) they can all view the same object or (c) can be divided into groups to target and track different objects at different angles and distances.

## MOTIVATION

Our proposed research is motivated by two fundamental challenges studied in two separate disciplines:

- **Challenge in image sensing:** lack of versatile camera systems in a small form factor.
- **Challenge in image understanding:** lack of algorithms that can recognize a generic 3D scene/object from 2D photos.

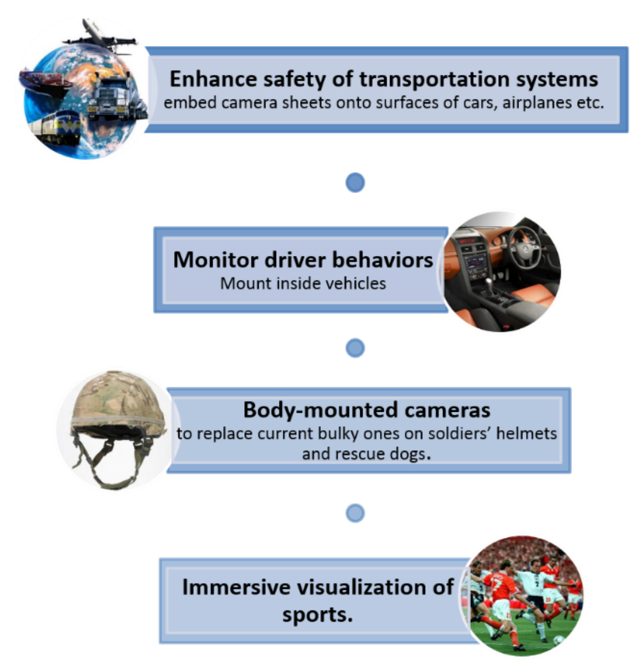


Fig 2. Potential target applications of our cyber-physical imaging system.

## RESEARCH PLAN

The premise of our proposal is that the aforementioned challenges can be more effectively addressed if we solve them together than tackle them separately.

### Hardware Implementation Strategy

- Fabrication of variable-focus lenses for the micro-cameras.
- Develop light concentrators for enhanced collection and concentration of light to compensate for small lens apertures.
- Design efficient micro-scale actuators for on-demand direction control of the cameras.
- Realize the flexible camera sheet using batch fabrication techniques.

### Software Implementation Strategy

- Develop efficient algorithms to combine noisy image data from multiple cameras into a single sharp image.
- Design new software to integrate the processes of depth estimation and object/scene recognition.
- Use human-user interaction to train the new model for generic object/scene recognition with minimum supervision.

## CURRENT PROGRESS

### Electrowetting Lenses

Designed and fabricated an array of electrowetting lens on flexible substrate

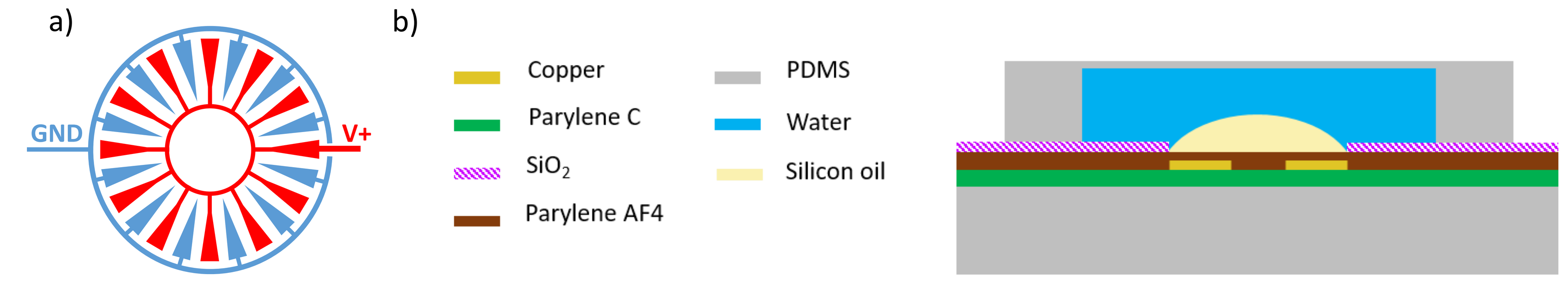


Fig 3. (a) Simple schematic of basic electrode design for a single electrowetting lens. The design works to both actuate and center the silicone oil droplet which forms the liquid lens. (b) Schematic of a cross section of a single device on the flexible array. This device is repeated across the substrate for form the full array.

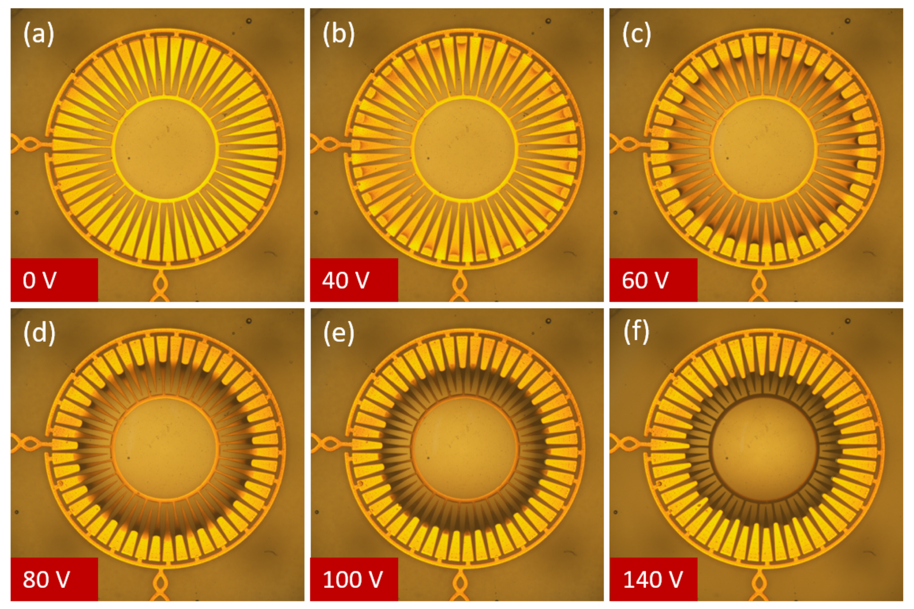


Fig. 4. Top view of the actuation of the lens. Darker, central region is silicon oil, surrounding medium is water. (a)The initial position of the oil droplet (with 0V applied). (b) Oil droplet begins to squeeze (resulting in decreased focal length) when 40V AC square wave (10kHz) is applied across underlying electrodes. (c)-(f) Focal length continues to decrease with increasing applied voltage.

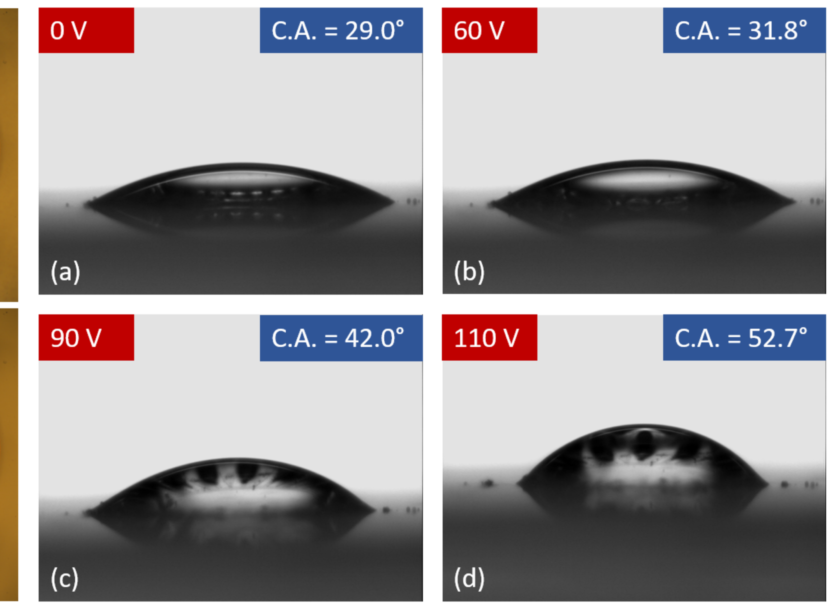


Fig. 5. Profile view of oil droplet taken on goniometer to show changing contact angle (C.A.). (a)The initial position of oil droplet (with 0V applied), with a corresponding contact angle of 29.0° (b) 60V with 31.8° contact angle. (c) 90V with 42.0° contact angle. (d) 110V with 53.7° contact angle.

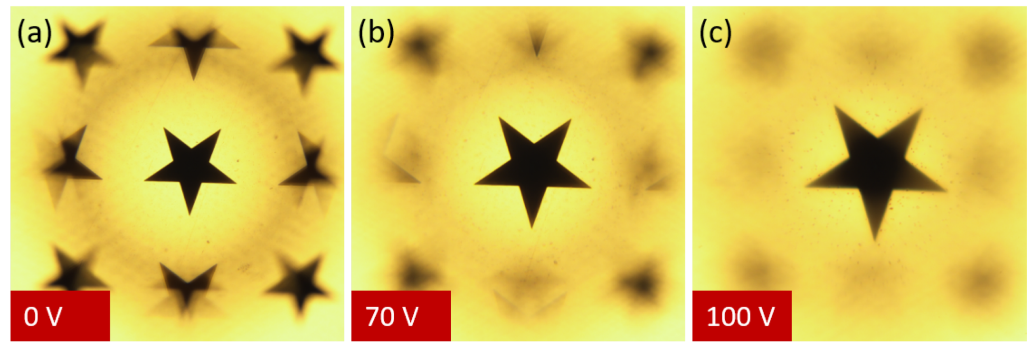


Fig. 6. The electrowetting lens viewed under the microscope is used to form an image from an object under the lens composed on an array of stars. (a) Initial image (b) Magnified image formed when the focal length decreases at 70V. (c) Further magnification of image which results from additional shortening of focal length at 100V.

Fig. 7. (a) 5 x 5 array of electrowetting lenses shown on the silicon carrier wafer used during the fabrication process for the flexible microlens array. (b) A close up showing a closer view of the electrodes and contacting pads for applying voltage to the array. (c) The full flexible (PDMS) array after peel off from the carrier wafer. It is shown wrapped on a transparent cylinder of with 75mm diameter. (d) A photograph showing the detail of the lenses' interdigitated electrodes which allow actuation. Also shown are the contact pads for applying ground and positive voltage across the device.

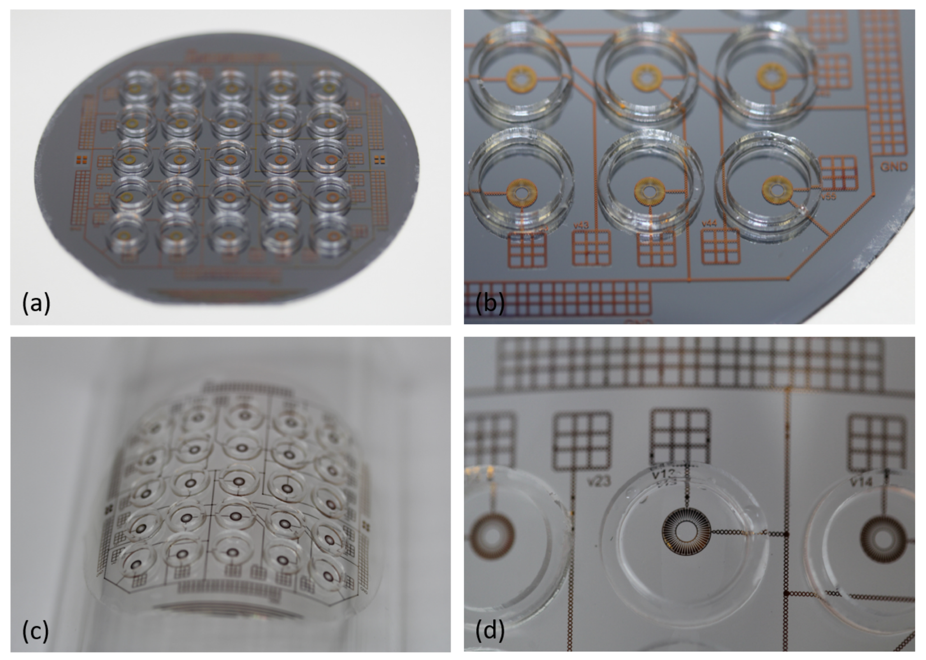


### Image Processing

Developed multi-view image denoising algorithm based on a data structure called 3D focus image stacks with robust disparity estimation and CNN-based denoising (in preparation of paper submission)

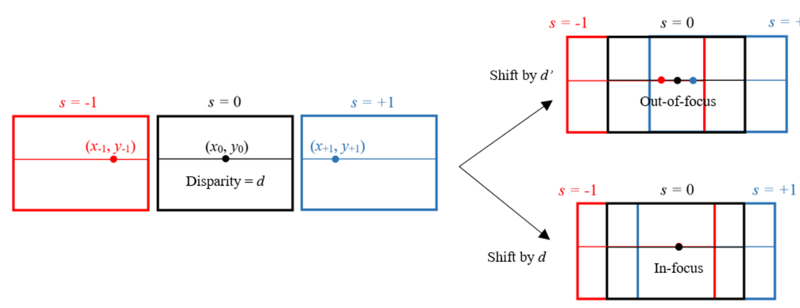


Fig 8. Construction of 3D focus image stacks. Multi-view images are shifted and stacked using different disparity values. Pixels with the correct disparity will for m a clear image, while pixels with incorrect disparities will appear as blur.

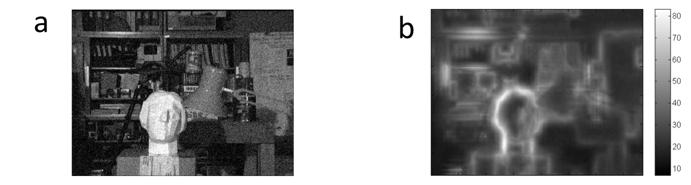


Fig 9. (a) Noisy image; (b) texture map estimated from 3D focus image stacks.

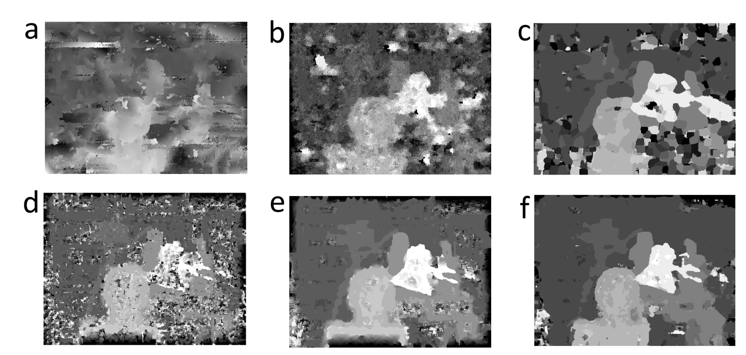


Fig 10. Texture-based disparity maps compared to other methods when noise $\sigma = 20$: (a) Taniai et al.; (b) Lee et al.; (c) Klaus et al.; (d) Miyata et al.; (e) our previous result; (f) proposed.

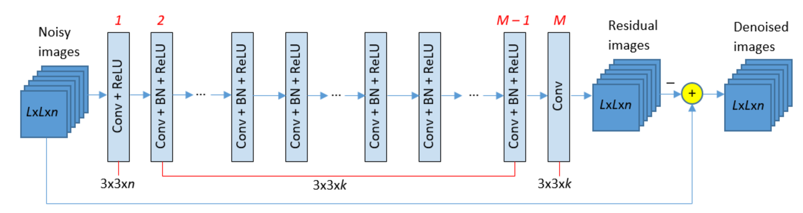


Fig 11. Proposed MVCNN model. Conv: convolution filter; BN: batch normalization; ReLU: rectified linear unit

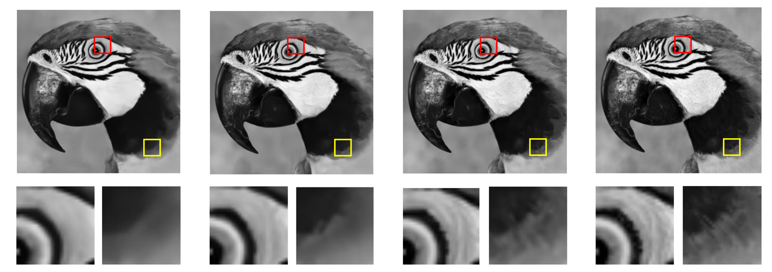

Fig 12. CNN denoising on sample image. From left to right: single image, 3 views, 9 views, and ground truth.

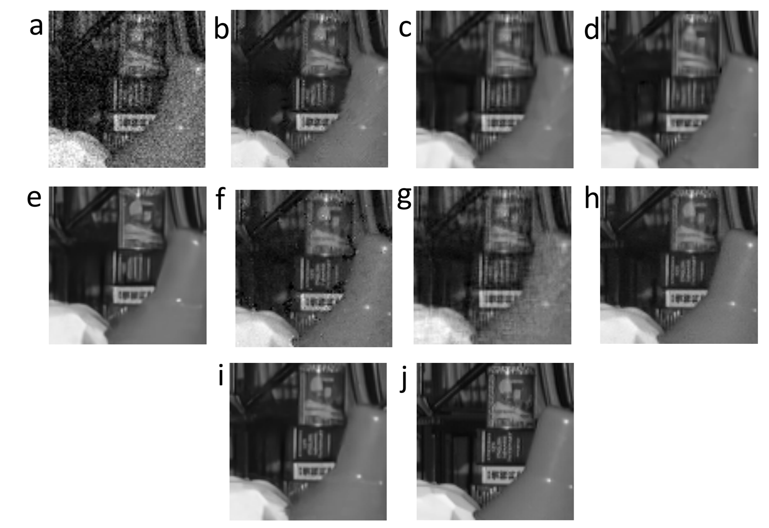


Fig 13. Comparison of denoising performance: (a) noisy image; (b) NLM; (c) BM3D; (d) WNNM; (e) DnCNN; (f) Miyata et al.; (g) VBM4D; (h) our previous work; (i) proposed MVCNN; (j) ground truth.

### LCE Microactuator and Magnetic Lenses

Liquid crystal elastomer (LCE) microactuator development for image tracking uses and Magnetically actuated lens design as possible alternative to Electrowetting

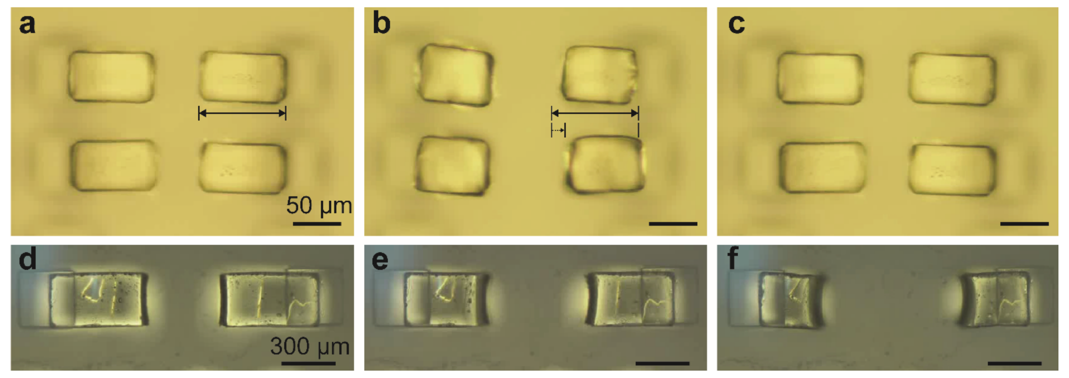


Fig 14. Demonstration of LCE microactuators showing showed two different actuation modes, contraction and bending. (a-c) Show a reversible contraction test with heating at (a) 50 °C, (b) 120 °C, (c) 50 °C. (d-f) Show a test of the bending motion with increasing heating at (d) 50 °C, (e) 90 °C, and (f) 120 °C.

Fig 15. (a) Cross section of the magnetically actuated liquid tunable lens. Radial magnetic fields are shown as dashed lines and arrows in the magnet show the direction of the field. Cross and dot in the winding show current direction. (b) the lens in the actuated state, which shows a deformed membrane (and thus a tunable lens) in the middle.

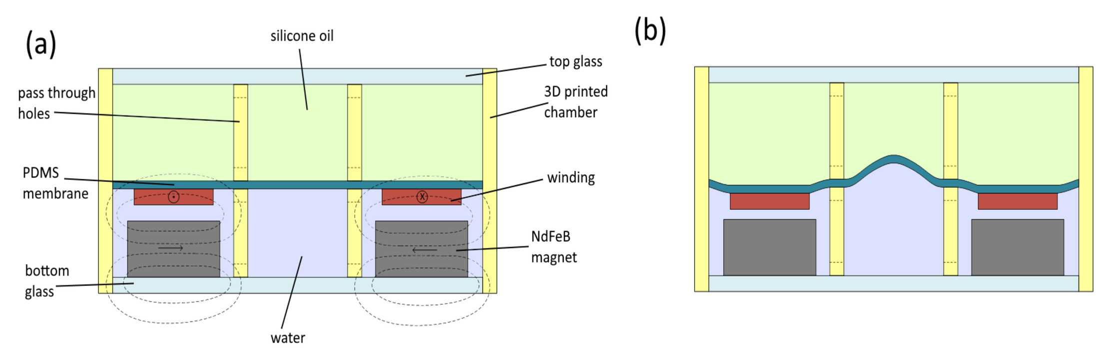


## ACKNOWLEGMENT

This work is funded by National Science Foundation under Cyber-Physical Systems (CPS) program award no. 1329481

## CONTACT INFORMATION

Dr. Hongrui Jiang
Department of Electrical and Computer Engineering
University of Wisconsin - Madison
Phone: (608) 265-9418 ; Email: hongrui@engr.wisc.edu

Micro-Nano Sensors and Actuators Lab MNSA